OXFORD GENETICS

GENETICS, 2023, 225(3), iyad162
https://doi.org/10.1093/genetics/iyad162
Advance Access Publication Date: 9 October 2023
Investigation

Variation in transcription regulator expression underlies differences in white–opaque switching between the SC5314 reference strain and the majority of *Candida albicans* clinical isolates

Matthew B. Lohse, Naomi Ziv, Alexander D. Johnson*

Department of Microbiology and Immunology, University of California - San Francisco, San Francisco, CA 94143, USA

*Corresponding author: Department of Microbiology and Immunology, University of California - San Francisco, 600 16th Street, Genentech Hall - N372, San Francisco, CA 94143, USA. Email: ajohnson@cgl.ucsf.edu

Candida albicans, a normal member of the human microbiome and an opportunistic fungal pathogen, undergoes several morphological transitions. One of these transitions is white–opaque switching, where *C. albicans* alternates between 2 stable cell types with distinct cellular and colony morphologies, metabolic preferences, mating abilities, and interactions with the innate immune system. White-to-opaque switching is regulated by mating type; it is repressed by the a1/α2 heterodimer in a/α cells, but this repression is lifted in a/a and α/α mating type cells (each of which are missing half of the repressor). The widely used *C. albicans* reference strain, SC5314, is unusual in that white–opaque switching is completely blocked when the cells are a/α; in contrast, most other *C. albicans* a/α strains can undergo white–opaque switching at an observable level. In this paper, we uncover the reason for this difference. We show that, in addition to repression by the a1/α2 heterodimer, SC5314 contains a second block to white–opaque switching: 4 transcription regulators of filamentous growth are upregulated in this strain and collectively suppress white–opaque switching. This second block is missing in the majority of clinical strains, and, although they still contain the a1/α2 heterodimer repressor, they exhibit a/α white–opaque switching at an observable level. When both blocks are absent, white–opaque switching occurs at very high levels. This work shows that white–opaque switching remains intact across a broad group of clinical strains, but the precise way it is regulated and therefore the frequency at which it occurs varies from strain to strain.

Keywords: *Candida albicans*; *BRG1*; *SFL2*; *UME6*; *RFX2*; white–opaque switching; mating type

Introduction

The fungal species *Candida albicans* is a common commensal member of the healthy human microbiome; *C. albicans* is also an opportunistic pathogen that can cause diseases ranging from yeast infections and thrush to systemic bloodstream infections with fatality rates exceeding 40% in individuals with compromised immune systems (Kennedy and Volz 1985; Wey *et al.* 1988; Wenzel 1995; Calderone and Fonzi 2001; Kullberg and Oude Lashof 2002; Eggimann *et al.* 2003; Gudlaugsson *et al.* 2003; Pappas *et al.* 2004; Achkar and Fries 2010; Kim and Sudbery 2011; Kumamoto 2011). *C. albicans* undergoes several morphological programs including the yeast–hyphal transition, chlamydospore formation, and white–opaque switching, where it alternates between 2 cell types with distinct cellular and colony morphologies (Slutsky *et al.* 1987; Soll *et al.* 1993; Johnson 2003; Pujol *et al.* 2004; Lohse and Johnson 2009; Soll 2009; Morschhäuser 2010; Porman *et al.* 2011). Switching between the white and opaque cell types is reversible, occurs without any chromosomal rearrangements or DNA sequence changes, and is notable for the stability of each of the 2 cell types formed: under lab conditions and in mouse models, each cell type is stable for many cell division cycles. Switching is stochastic and occurs approximately once every 10^4 cell divisions under standard laboratory conditions (Rikkerink *et al.* 1988; Bergen *et al.* 1990; Takagi *et al.* 2019; Beekman *et al.* 2021). The white–opaque switching frequency responds to environmental signals, such as elevated temperature (Slutsky *et al.* 1987; Rikkerink *et al.* 1988) or exposure to N-acetylglucosamine (GlcNAc) (Huang *et al.* 2010), which can drive switching in 1 direction or the other. Approximately one-sixth of the *C. albicans* transcriptome is differentially expressed (at least 3-fold) between the 2 cell types (Lan *et al.* 2002; Tuch *et al.* 2010); this results in the 2 cell types having distinct metabolic preferences (Lan *et al.* 2002; Ene *et al.* 2016; Lohse *et al.* 2020), mating abilities (Lockhart *et al.* 2002; Miller and Johnson 2002), interactions with the innate immune system (Kvaal *et al.* 1997, 1999; Geiger *et al.* 2004; Lohse and Johnson 2008; Sasse *et al.* 2013), abilities to colonize and persist in host organs (Takagi *et al.* 2019), and responses to environmental cues (Hornby *et al.* 2001; Dumitru *et al.* 2007; Si *et al.* 2013; Sun *et al.* 2015). White–opaque switching is controlled by a circuit of 8 transcriptional regulators connected by interlocking feedback loops; the most important regulator is Wor1, which is needed for both the establishment and the continued maintenance of the opaque cell type (Sonneborn *et al.* 1999; Srikantha *et al.* 2000; Huang *et al.* 2006; Srikantha *et al.* 2006; Zordan *et al.* 2006; Vinces and

Received on 27 July 2023; accepted on 26 August 2023

Kumamoto 2007; Zordan *et al.* 2007; Wang *et al.* 2011; Hernday *et al.* 2013; Lohse *et al.* 2013; Hernday *et al.* 2016; Lohse and Johnson 2016; Rodriguez *et al.* 2020). Given the responsiveness of white–opaque switching to environmental signals, it is not surprising that the Cek1 MAP kinase (Ramírez-Zavala *et al.* 2013; Deng and Lin 2018), cAMP/protein kinase A (Ramírez-Zavala *et al.* 2013; Ene *et al.* 2016; Cao *et al.* 2017; Ding *et al.* 2017), and Hog1 (Liang *et al.* 2014; Deng and Lin 2018; Correia *et al.* 2020) signaling pathways, as well as roughly 20% of gene deletions tested in 2 systematic screens (Lohse *et al.* 2016; Brenes *et al.* 2020), affect switching between the 2 cell types in 1 or both directions. Thus, the regulation of white–opaque switching appears to be a hub responsive to many different signals.

Following the discovery of *C. albicans* mating and the identification of 4 transcriptional regulators controlling the mating type programs (MTLa1, MTLa2, MTLα1, and MTLα2) (Hull and Johnson 1999; Hull *et al.* 2000; Magee and Magee 2000; Tsong *et al.* 2003), work with several strains, including the commonly used SC5314 reference strain (that is, the strain most commonly used in laboratory settings and the source of the initial *C. albicans* genome sequence), showed that a/a or α/α strains, but not a/α stains, could form opaque cells (Lockhart *et al.* 2002; Miller and Johnson 2002). A mechanism underlying this cell type dependence became apparent once Wor1 was identified as the key regulator of the opaque cell type: the MTLa1/MTLα2 transcriptional regulator heterodimer binds to the *WOR1* promoter in a/α cells, repressing it and preventing switching. Because a/a and α/α cells each produce only half of the repressor, *WOR1* is expressed, and switching can occur (Lan *et al.* 2002; Huang *et al.* 2006; Srikantha *et al.* 2006; Zordan *et al.* 2006). More than 90% of *C. albicans* isolates tested are a/α, as opposed to a/a or α/α (Odds *et al.* 2007), and this observation raised questions about the relevance of white–opaque switching because most strains were, like SC5314, assumed to be incapable of forming opaque cells without first undergoing a change in mating type. It was subsequently discovered, using a different set of in vitro conditions (GlcNAc and CO_2), that up to two-thirds of clinical *C. albicans* a/α isolates were, in fact, capable of forming opaque cells (Xie *et al.* 2013; Hu *et al.* 2016; Li *et al.* 2016; Park *et al.* 2020). Despite the identification of these opaque-promoting conditions, SC5314 a/α cells still appear unable to form opaque cells. In this paper, we address the cause of this difference between SC5314 and other switching competent a/α strains.

Materials and methods

Growth conditions

Unless otherwise noted, strains were grown, and assays were performed on synthetic complete (SC) defined media plates containing yeast nitrogen base with 0.5% ammonium sulfate (6.7 g/L, BD #291940), amino acids (2 g/L), uridine (100 μg/mL), 2% glucose, and 2% agar (SCD + aa + Uri); 2% GlcNAc (Sigma #A3286) was added instead of glucose when relevant (SCGlcNAc + aa + Uri) and liquid media omitted agar. Growth in ambient air was conducted in an incubator at 25°C. Growth in 5% CO_2 was conducted in either a HERAcell VIOS 160i (Thermo Scientific) incubator at 25°C or in an anaerobic chamber (COY Lab Products) set to 21% O_2 and 5% CO_2 at room temperature (~22°C).

Plasmid construction

Lists of plasmids and oligonucleotides used in this study can be found in Supplementary File 1.

The p*CAG1*-mCherry (mCherry-*SAT1-RPS1*) reporter plasmid was constructed in the previously reported pNZ116 backbone (Lohse *et al.* 2020). The promoter for *CAG1* (499 bp) was amplified from *C. albicans* SC5314 genomic DNA and added to HindIII digested pNZ116 backbone using In-Fusion Cloning (Takara #638911) to generate plasmid pNZ141. The resulting plasmid was then linearized by AgeI digestion prior to transformation into *C. albicans*. The promoter region used in this construct extends from just upstream of the ATG at the start of *CAG1* to 305 bp inside the 3′ end of the upstream gene (C5_05210W/orf19.4014). We used a promoter extending into the upstream gene due to the small size of the C5_05210W-*CAG1* intergenic region (194 bp) and the close proximity of the a1/α2 binding motif to the 3′ end of the upstream gene (roughly 25 bp).

The MTL deletion plasmid, a SAT1-based equivalent to the previously published Arg4-based pJD1 (Lin *et al.* 2013), was constructed as follows. The 500-bp 5′ and 3′ of the MTL locus were PCR-amplified, fused together with XhoI and NotI restriction sites positioned between them, and integrated between the SphI and AatII sites of pUC19 to form pMBL743. During this process, a pair of XmaI sites was added just inside the SphI and AatII sites to allow for easier linearization of the final construct. The nonrecyclable version of the SAT1 marker from pMBL180 (Lohse and Johnson 2016) was then PCR-amplified and integrated into pMBL743 between the XhoI and NotI sites to form pMBL744. The resulting plasmid was then linearized by XmaI digestion prior to transformation into *C. albicans*.

The p*ENO1*-Cas9-t*CYC1* plasmid for CRISPR-based gene deletions independent of the requirement for heterozygous *leu2* deletion was constructed by modifying pADH140 (Nguyen *et al.* 2017) in order to introduce StuI sites on both flanks of the P_{ENO1}-CAS9-t_{CYC1} region. Briefly, a partial P_{ENO1}-CAS9 fragment was PCR-amplified from pADH140 by AccuPrime pfx (Invitrogen). To add StuI sites, the replication origin, ampicillin marker, t_{CYC1}, and partial P_{ENO1} fragments were independently PCR-amplified from pADH140. These 3 PCR products were then fused, amplified by PCR, and the resulting product linked with the initial P_{ENO1}-CAS9 fragment by In-Fusion seamless cloning (Takara) to form pp2280. This plasmid was linearized by StuI digestion prior to transformation into *C. albicans*.

Strain construction

Lists of strains, plasmids, and oligonucleotides used in this study can be found in Supplementary File 1.

C. albicans a/α SC5314 was isolated from a patient with a *Candida* infection prior to 1968 (Aszalos *et al.* 1968; Maestrone and Semar 1968; Meyers *et al.* 1968), and its derivatives served as a basis for comparison to other isolates as well as the template for constructing several deletion strains. Unmodified SC5314 served as the template for constructing the new *brg1*, *rfx2*, *sfl2*, and *ume6* single and combination deletion strains as well as the control a/Δ and α/Δ strains used for comparisons to other derived a/Δ and α/Δ strains. The SC5314-derived *C. albicans* wild-type a/α SN250 and OHY13 (*HIS1-LEU2*) and SN425 (*HIS1-LEU2-ARG4*) addbacks to the SN152 a/α *his1 leu2 arg4* strain have been previously reported (Noble and Johnson 2005; Homann *et al.* 2009). The single *brg1*, *rfx2*, *sfl2*, and *ume6* deletion a/α strains used for NanoString transcriptional profiling have been previously reported (Banerjee *et al.* 2008; Homann *et al.* 2009; Fox *et al.* 2014), and the aforementioned OHY13 addback strain served as a control for experiments using those strains.

Several of the a/α strains used, as well as some of the a/a and α/α strains used as controls for the flow cytometry experiments, were taken from a set of 20 strains that have previously been sequenced (Hirakawa *et al.* 2015) and used for MTL heterozygosity

studies in animal models (Wu *et al.* 2007). Many of these strains were initially identified and characterized during studies of clinical isolates (Lockhart *et al.* 1996, 2002; Blignaut *et al.* 2002; Pujol *et al.* 2002). The remainder of the a/α strains used in this study are from the set of clinical isolates profiled in the initial a/α opaque cell formation report (Xie *et al.* 2013); we selected a mixture of strains reported to be capable and incapable of a/α opaque cell formation from the larger set. Two of the strains we profiled from this set (JX1348/ci28 and JX1353/ci32) were reported to be MTL a/a and α/α, respectively; however, our characterization of these strains by colony PCR (and NanoString, for JX1353/ci32) indicates that they are both MTLa/α. Regardless of the cause of this discrepancy, both these strains were capable of a/α opaque cell formation in our hands. A guide to the mCherry reporter-tagged strains, a/Δ or α/Δ derivatives of a/α strains, and opaque cell derivative strains (a/α, a/Δ, and α/Δ) can be found in Supplementary File 1.

The mCherry reporter strains were constructed using AgeI-HF (NEB R3552L) linearized pNZ141 transformed into the relevant parent strains. Plasmid integration at the *RPS1* (*RP10*) locus was verified by colony PCR across the 5′ and 3′ flanks of the integrated plasmid. Conversion of a/α strains to the a/Δ or α/Δ mating type utilized XmaI-digested pMBL744; loss of 1 MTL copy was verified by colony PCR. Whenever possible, the a/Δ strain background was used instead of the α/Δ strain background. Opaque cells were isolated for the resulting a/Δ and α/Δ strains during the course of white-to-opaque switching assays as described below.

The new single and combination *brg1*, *rfx2*, *sfl2*, and *ume6* deletion strains used for switching assays were constructed sequentially in the previously unmodified a/α SC5314 background using a modification of the protocol described by Huang *et al.* (2021). For these deletions, the donor DNA (dDNA) contains homology to the regions immediately upstream and downstream of the gene being deleted and was PCR-amplified from pADH34 (Hernday *et al.* 2010) in order to contain the maltose-recyclable *SAT1* marker. The gRNA site was selected from options suggested by Benchling and compared to the list of unique guide sequences developed by Vyas *et al.* (2015) in order to ensure specificity to the desired location; once a gRNA sequence was chosen, the P_{SNR52}-gRNA-scaffoldTerminator construct was created through PCR amplification of 2 fragments from pADH143 (Nguyen *et al.* 2017) followed by a subsequent round of PCR to fuse the 2 fragments. The P_{ENO1}-Cas9-T_{CYC1} construct was prepared by StuI-digesting the pp2280 plasmid. The 3 constructs were transformed into a/α SC5314 and plated on YPD plus 400 µg/mL nourseothricin. Gene deletions were verified by colony PCR reactions verifying loss of the targeted gene and proper integration of the *SAT1* knockout cassette. The *SAT1* knockout cassette was recycled by overnight growth in YEP media supplemented with 2% maltose, after which cells were plated on YPD plus 25 µg/mL nourseothricin for 24 h to identify small colonies which had lost the *SAT1* marker and replated on YPD plus 400 µg/mL nourseothricin to verify loss of the *SAT1* marker. Marker excision and absence of targeted genes were then verified by an additional round of colony PCR. In the case of combination deletions, the absence of all expected genes was verified at each step in the process. For these strains, the order of genes in the description represents the order in which genes were deleted, as such strains with the same genes in a different order (e.g. *brg1*-*sfl2* and *sfl2*-*brg1*) are independently constructed versions of a deletion strain for those genes.

Flow cytometry

Overnight cultures of pCAG1-mCherry reporter strains were started from 2-day-old YPD + Ade plates; all cultures were 2 mL of SCGlcNAc + aa + Uri in a well of a 24-deep well plate that was sealed with Breathe-Easy sealing membranes (Diversified Biotech, BEM-1) and agitated at 200 rpm at 25°C in a Excella E25 Incubator (New Brunswick Scientific). Overnight, cultures were then diluted back 1:10 in fresh media and agitated for ∼5 h. Fluorescence was measured using a BD FACS Celesta with a 488-nm laser with a 530/30 bandpass filter and a 561-nm laser with a 610/20 bandpass filter. Samples were loaded from 5-mL tubes (Falcon 352052), and normal acquisition was 10,000 events for each strain on the high setting. Data for each sample were exported as an FCS file, and all subsequent analyses were done with R (version 4.0.2) (R Core Team 2019) using the flowCore (version 2.2.0) (Ellis *et al.* 2019), ggcyto (version 1.18.0) (Van *et al.* 2018), and tidyverse (version 1.3.0) (Wickham 2017) packages.

NanoString

Transcriptional analysis was conducted using NanoString probes against a set of 68 *C. albicans* genes and both strands of the short and long *WOR1* 5′ UTRs (1 probe per gene or UTR, 72 probes total). Probes were designed and synthesized by NanoString Technologies. A list of target genes and probe sequences can be found in Supplementary File 2.

Cultures of strains being profiled were most commonly grown in SCGlcNAc + aa + Uri with 5% CO_2; when needed, cultures were grown in SCD + aa + Uri and/or ambient air. Cultures were 2 mL in 24-deep well format plates sealed with Breathe-Easy sealing membranes (Diversified Biotech, BEM-1). Ambient air cultures were agitated at 200 rpm at 25°C in a Excella E25 Incubator (New Brunswick Scientific), and CO_2 cultures were agitated at 600 rpm at 25°C in an Incu-Mixer MP shaker (Benchmark) placed in an anaerobic chamber (COY Lab Products) set to 21% O_2 and 5% CO_2 at room temperature (∼22°C). Overnight cultures were diluted back between 10-fold and 50-fold into fresh media and allowed to grow for ∼5 h. At this point, 1.5 mL of each strain was centrifuged, decanted, and flash frozen before storing at −80°C. During the harvesting process, a small aliquot of each sample was plated to determine the white–opaque composition of each culture. Total RNA was extracted using a MasterPure Yeast RNA Purification Kit (Lucigen MPY03100), RNA concentration was then determined using a Qubit RNA BR Kit and Qubit Fluorometer (Molecular Probes/Life Technologies), and RNA quantity was normalized to a concentration of 20 ng/µL in a volume of at least 20 µL. Samples were processed on a nCounter Sprint Profiler (NanoString Technologies) at the LCA-Genome Core Facility at the University of California, San Francisco. Read count data were processed using the nSolver analysis software (NanoString Technologies). Two independent replicates were analyzed for each sample except for a/α SC5314 on GlcNAc with 5% CO_2; in this case, 4 replicates were analyzed.

Raw counts were exported from nSolver (version 4.0.70) and then normalized with R (version 4.0.2) (R Core Team 2019) using the tidyverse package (version 1.3.0) (Wickham 2017). All data were normalized based on 5 housekeeping genes [*PGA59*, *TBP1*, *HTA1*, *PAT1* (C4_04870C), and *DYN1*]. The geometric mean of these 5 housekeeping genes for each sample was calculated, and the difference between the geometric mean of these housekeeping genes across all samples and the geometric mean of these 5 housekeeping genes in each individual sample was determined. This difference was then subtracted from all reads in that individual sample to normalize the data, and these normalized read counts were used for all further comparisons and analyses. Student's t-tests (2-tailed, assuming unequal variance) were performed on the normalized average read counts for each gene to compare

between the switching-capable and switching-incapable strains. Significance was evaluated using a 5% false discovery rate (with Bonferroni correction for multiple testing). Raw and normalized NanoString data can be found in Supplementary File 2 and are also available as accession number GSE241766 at the NCBI GEO.

Switching assays

White-to-opaque and opaque-to-white switching assays followed previously reported protocols with modifications where needed (e.g. incubation with 5% CO_2) (Miller and Johnson 2002; Zordan *et al.* 2007; Lohse *et al.* 2016). In brief, strains were allowed to recover from glycerol stocks on SCD + aa + Uri (white cells and some opaque cells) or SCGlcNAc + aa + uri (most opaque stability assays) plates at 25°C. After 6 or 7 days, 5 colonies per strain that lacked visible sectors of the other cell type were resuspended in water and plated at a concentration of ~100 colonies/plate. Unless otherwise noted, plates were incubated for 5–7 days at 25°C in ambient air before scoring.

The most common assay setups were as follows. For a/α white-to-opaque switching assays, we tested SCGlcNAc + aa + Uri (CO_2 and air) and SCD + aa + Uri (air), usually with 5 plates per condition–strain pairing. For a/Δ and α/Δ white-to-opaque switching assays, we tested SCGlcNAc + aa + Uri (air) and SCD + aa + Uri (air), usually with 5 plates per condition–strain pairing. The a/Δ and α/Δ strains that did not give rise to opaque cells in this initial assay were then tested again with 10 SCGlcNAc + aa + Uri plates (CO_2). For transcriptional regulator deletion strain white-to-opaque switching assays, we normally tested 5 SCGlcNAc + aa + Uri plates (air and CO_2). For opaque stability assays (a/α, a/Δ, and α/Δ), we used 2 plates each of SCGlcNAc + aa + Uri (air) and SCD + aa + Uri (air).

Three phenotypes were noted during the scoring process: (1) the number of sectored colonies, (2) the number of fully switched colonies, and (3) the total number of colonies. The total number of colonies was determined using an aCOLyte^3 colony counter (Synbiosis), and colony morphology and sectoring were determined by manual observation. For white-to-opaque switching assays, the switching frequency was calculated as 100 * (number of sectored colonies + number of fully switched colonies)/total number of colonies; this metric considers all possible switching events. For opaque stability assays (opaque-to-white switching), the stability rate was calculated as 100 * (number of fully unswitched (opaque) colonies + number of sectored colonies)/total number of colonies; this metric considers all colonies with at least some visible opaque cells as having at least some opaque stability. If no switching events (white-to-opaque assay) or opaque-containing colonies (opaque stability) were observed, the rate is reported as less than 100/total number of colonies.

Results

General defects in MTLa1/MTLα2 repression do not explain a/α opaque formation

A plausible hypothesis to explain the ability of many *C. albicans* a/α strains to switch to the opaque cell type is that these strains have a defect in the expression or function of the transcriptional regulators MTLa1 and/or MTLα2 resulting in increased expression of MTLa1/MTLα2-repressed genes (including *WOR1*) in a/α cells. To test this hypothesis across a diverse set of a/α strains, we constructed a reporter where the *CAG1* upstream regulatory region controls mCherry expression, integrated this reporter into 53 a/α strains selected to include both switching-capable and switching-incapable ones (including SC5314), and measured mCherry expression by flow cytometry. The *CAG1* regulatory region was chosen because it (1) is bound by MTLa1 and MTLα2, (2) is repressed 10-fold in a/α cells relative to **a** and α cells, and (3) its expression is not white or opaque cell-type dependent. We found that mCherry levels did not consistently differ between the switching-capable and switching-incapable a/α strains (including SC5314), thereby ruling out this hypothesis (Fig. 1a).

Targeted transcriptional profiling for hypothesis evaluation

Having ruled out the MTLa1/MTLα2-repression defect hypothesis, we next turned to targeted transcriptional profiling to search for gene expression changes that could explain the differences in the regulation of switching. We designed a 72-probe NanoString library targeting 68 different genes implicated in white–opaque switching. We used this probe set to track gene expression in SC5314 and 16 other a/α strains, 9 of which could undergo white–opaque switching in our hands, in liquid SCGlcNAc + aa + Uri media with 5% CO_2. It is readily apparent that expression of the profiled genes does not significantly differ ($P > 0.05$ post-Bonferroni correction) between the 9 a/α strains that formed opaques and the 7 a/α strains that did not form opaques (Fig. 1b; Supplementary File 2). Consistent with our earlier results, we note that expression of MTLa1 and MTLα2 does not significantly differ between the switching-capable and switching-incapable a/α strains (Supplementary Fig. 1 and File S2). However, there was a large difference between SC5314 and the remaining 16 strains, regardless of the latter's ability to form a/α opaques (Fig. 1c; Supplementary File 2). This result suggests that, in the presence of GlcNAc and CO_2, SC5314 is an outlier relative to all other strains tested. The largest expression difference between SC5314 and the other strains was observed for 4 of the genes we tested: mRNA levels of *BRG1* were 13-fold higher, *UME6* were 8-fold higher, *RFX2* were 5-fold higher, and *SFL2* were 3-fold higher in SC5314 relative to the other 16 a/α strains (Fig. 1d; Supplementary File 2). Expression of these 4 genes did not differ among the 16 non-SC5314 strains (Fig. 1d; Supplementary File 2). We also note that the high expression of these genes in SC5314, relative to the other strains, persists when the strains are switched to the **a** or α mating types (Supplementary Fig. 2 and File S2).

SC5314 has an abnormally high filamentation response to GlcNAc and CO_2

The 4 genes expressed at higher levels in SC5314 relative to the other a/α strains encode transcriptional regulators. Three (*BRG1*, *SFL2*, and *UME6*) are known to promote filamentous growth and 1 (*RFX2*) to repress it (Banerjee *et al.* 2008; Carlisle *et al.* 2009; Hao *et al.* 2009; Homann *et al.* 2009; Zeidler *et al.* 2009; Spiering *et al.* 2010; Song *et al.* 2011; Cleary *et al.* 2012). More specifically, Brg1 and Ume6 have been linked to the induction of filamentation in response to the 2 environmental signals, GlcNAc and CO_2, which are those commonly used to induce a/α white–opaque switching (Naseem *et al.* 2011; Cleary *et al.* 2012; Lu *et al.* 2013, 2019; Mendelsohn *et al.* 2017; Su *et al.* 2018). Based on these observations, we determined whether the transcriptional differences between SC5314 and the other strains were dependent on GlcNAc and/or CO_2. To address this question, we transcriptionally profiled (1) SC5314 grown with pairwise combinations of glucose or GlcNAc and air or CO_2 and (2) 6 other a/α strains grown on glucose and ambient air. These experiments established that, in the absence of GlcNAc and CO_2, SC5314 exhibited a transcriptional profile similar to those of the other strains (Fig. 2a; Supplementary File 2). However, the results were different in GlcNAc and CO_2: in SC5314, *BRG1* is induced in response to either GlcNAc or CO_2, and

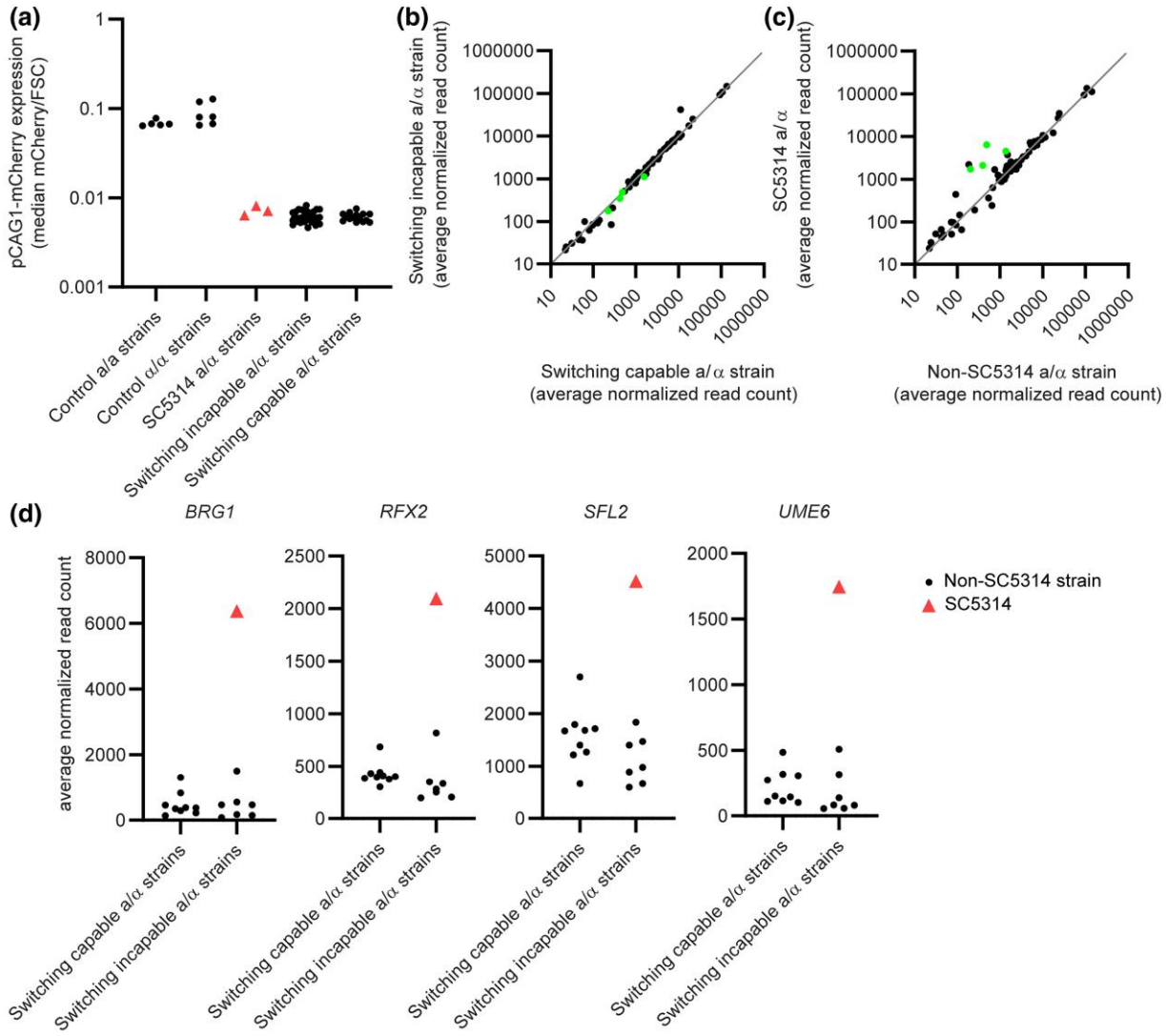

Fig. 1. SC5314 a/α has a distinct transcriptional profile from the other a/α strains. a) Normalized median fluorescence (mCherry/FSC) for a pCAG1-mCherry reporter in various a/a, α/α, and a/α strains grown on SGlcNAc + aa + Uri media. Each dot represents an individual strain; 3 different SC5314-derived a/α strains are included (red triangles). The y-axis is plotted on a log10 scale. b) Average normalized read counts for 72 NanoString probes in 9 switching-capable (x-axis) and 7 switching-incapable (y-axis) a/α non-SC5314 strains. *BRG1*, *RFX2*, *SFL2*, and *UME6* are indicated with green circles. Axes are plotted on a log10 scale, and the line of identity ($y = x$) is indicated. c) Average normalized read counts for 72 NanoString probes in 16 switching-capable and switching-incapable a/α non-SC5314 strains (x-axis) plotted vs SC5314 a/α (y-axis). *BRG1*, *RFX2*, *SFL2*, and *UME6* are indicated with green circles. Axes are plotted on a log10 scale and the line of identity ($y = x$) is indicated. d) Normalized read counts for *BRG1*, *RFX2*, *SFL2*, and *UME6* in 9 switching-capable and 8 switching-incapable (including SC5314) a/α strains. Non-SC5314 strains are indicated with black circles, SC5314 is indicated with a red triangle. Each point represents the average of all replicates for a given strain (4 for SC5314, 2 for all other strains).

SFL2, *UME6*, and *RFX2* were induced in response to GlcNAc but not CO_2 (Fig. 2b; Supplementary File 2). This induction was either not observed or observed to a lesser extent in the other strains (Supplementary Fig. 3 and File S2). In other words, SC5314 is similar to the other 6 strains on standard lab medium (glucose and ambient air) but is unique in strongly upregulating the 4 filamentation controlling genes in response to GlcNAc and CO_2, the conditions commonly used to promote a/α white-to-opaque switching.

No single regulator explains the difference between SC5314 and other strains

Several of the filamentation regulators identified by our transcriptional profiling have been reported to directly or indirectly affect each other's expression (e.g. Sfl2 induces *UME6* directly and *BRG1* indirectly through repression of *SFL1*; Znaidi *et al.* 2013). To determine if reduced expression of 1 of these regulators could explain the expression differences between SC5314 and the other strains, we transcriptionally profiled a/α SC5314 *brg1*, *sfl2*, *ume6*, and *rfx2* single deletion strains and found that Brg1 is needed for the high expression of *UME6* and *RFX2*, while Rfx2 represses *BRG1* and *UME6* expression (the latter either directly or indirectly through repression of *BRG1*) (Fig. 2c; Supplementary File 2). Conversely, deletion of *UME6* or *SFL2* did not affect expression of any of these 4 regulators, and none of the other deletions affected *SFL2* expression (Fig. 2c; Supplementary File 2). None of the single regulator deletions produced an expression profile comparable to the other a/α strains, suggesting that decreased expression of any one of these regulators cannot explain the transcriptional differences between SC5314 and the other strains.

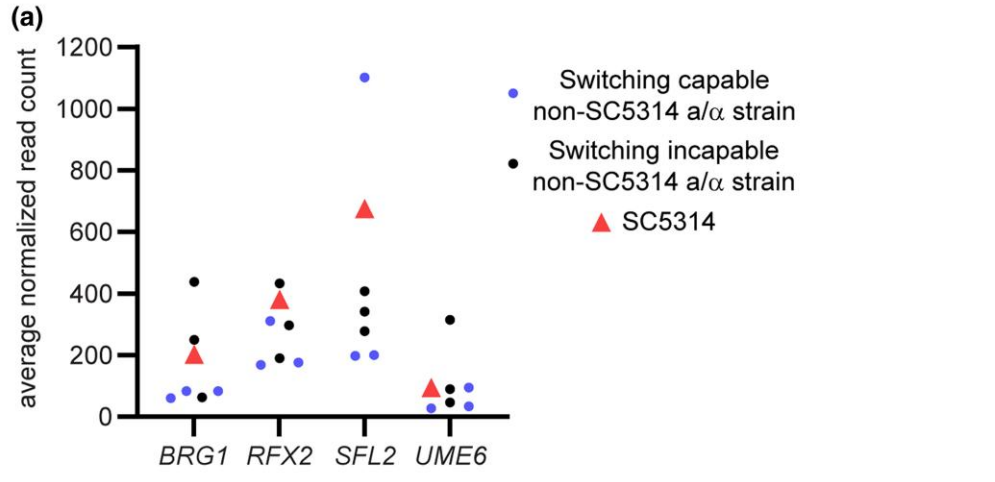

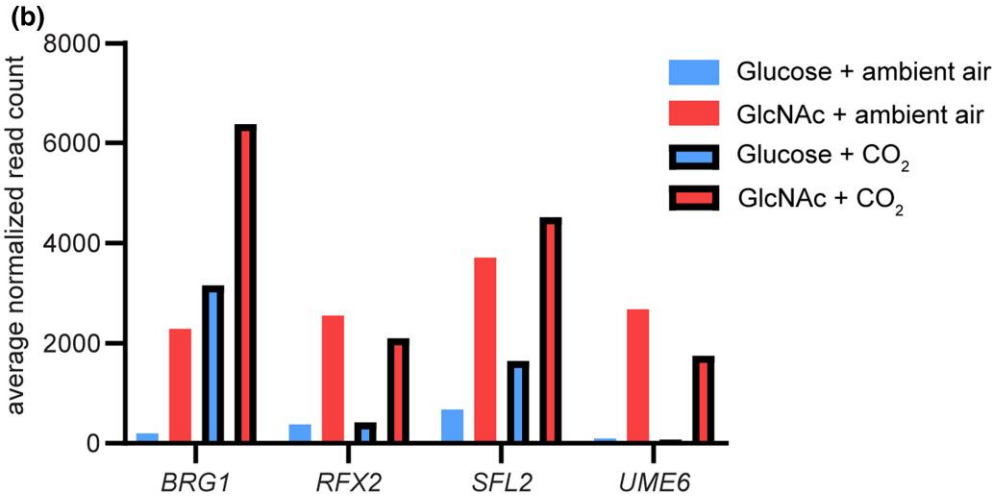

(c)

Fold change	Regulator deleted: BRG1	RFX2	SFL2	UME6
BRG1	-	+3.5	+1.4	1.0
RFX2	-3.1	-	1.0	-1.3
SFL2	-1.4	+1.8	-	-1.5
UME6	-5.6	+4.6	-1.6	-

Fig. 2. SC5314 a/α abnormally upregulates *BRG1*, *RFX2*, *SFL2*, and *UME6* in response to GlcNAc and CO_2. a) Average read counts for indicated genes in SC5314 a/α (red triangles) and 6 other a/α clinical strains (switching-capable strains are indicated with blue circles; switching-incapable strains are indicated with black circles) grown on glucose exposed to ambient air. Dots represent the average normalized read counts from 2 repeats for each strain. b) Normalized read counts for these 4 genes in SC5314 a/α when grown on glucose (blue) or GlcNAc (red) exposed to ambient air (clear bars) or CO_2 (bars with black outlines). Bars represent the average normalized read counts from 4 (SC5314 a/α on GlcNAc and 5% CO_2) or 2 repeats (all other strain/condition pairings) for each condition. c) Fold change in expression of the indicated regulator (left) in response to deletion of 1 of the 4 regulators (top). Values represent the average fold change, relative to wild type, from 2 repeats for each strain. Strains were grown on GlcNAc with 5% CO_2.

Multiple regulators contribute to SC5314 a/α opaque repression

Single deletions of *BRG1* and *SFL2* have been reported to allow for a/α SC5314 opaque cell formation (Xie *et al.* 2013; Park *et al.* 2019), and the remaining 2 (*RFX2*, *UME6*) have not, to the best of our knowledge, been tested for this phenotype. To verify and compare the reported *brg1* and *sfl2* results and to test the 2 uncharacterized regulator deletions, we constructed new, genetically matched deletions of these 4 genes in a/α SC5314. Consistent with previous reports, deletion of either *BRG1* or *SFL2* allowed for a/α opaque cell formation at a low rate (Table 1; Supplementary File 3). Conversely, we did not detect a/α opaque switching by either the *ume6* or *rfx2* deletions. We constructed all possible double, triple, and quadruple deletion combinations for these 4 genes. Certain combinations of double (e.g. *brg1-sfl2* and *brg1- rfx2*), triple (e.g. *brg1-sfl2-ume6*, *brg1-ume6-rfx2*, and *sfl2-ume6-rfx2*), and the quadruple deletion resulted in a/α opaque switching at rates that were higher than the single deletion strains, indicating that multiple regulators contribute to repression of a/α opaque switching in SC5314 (Table 1; Supplementary File 3). We note that the switching rates for these deletion strains tended to be higher in GlcNAc and 5% CO_2 (compared to GlcNAc and ambient air), indicating that both of these signals are needed for maximum switching.

Table 1. White-to-opaque switching rates for selected a/α SC5314 deletion strains on GlcNAc in ambient air or 5% CO_2.

	GlcNAc, ambient air		GlcNAc, 5% CO_2	
Strain	**white-to-opaque switching rate (%)**	***n***	**white-to-opaque switching rate (%)**	***n***
a/α wild type [a]	<0.10	996	<0.15	677
a/α brg1 deletion A isolate [a]	0.10	973	0.21	944
a/α sfl2 deletion A isolate [a]	0.10	1050	<0.12	858
a/α ume6 deletion A isolate [a]	<0.09	1098	<0.13	742
a/α rfx2 deletion A isolate	<0.28	361	<0.28	360
a/α brg1 sfl2 double deletion	0.45	443	0.21	481
a/α brg1 rfx2 double deletion	<0.17	575	0.18	552
a/α brg1 sfl2 ume6 triple deletion	<0.15	679	0.42	712
a/α ume6 rfx2 brg1 triple deletion	<0.18	551	0.37	546
a/α rfx2 ume6 sfl2 triple deletion	<0.19	527	3.51	598
a/α brg1 sfl2 ume6 rfx2 quad deletion	0.21	487	2.10	524
a/α sfl2 brg1 rfx2 ume6 quad deletion	<0.13	800	0.79	762
a/α ume6 rfx2 brg1 sfl2 quad deletion	0.14	738	1.19	758
a/α rfx2 ume6 sfl2 brg1 quad deletion	0.14	702	1.29	697

Data for additional deletion strains are presented in Supplementary File 3.
[a] Combined results for 2 independent assays with this strain.

Table 2. White-to-opaque switching rates for selected a/Δ SC5314 deletion strains on glucose in ambient air or GlcNAc in 5% CO_2.

	Glucose, ambient air		GlcNAc, 5% CO_2	
Strain	**white-to-opaque switching rate (%)**	***n***	**white-to-opaque switching rate (%)**	***n***
Wild-type a/Δ	0.53	567	0.49[a]	408
a/Δ brg1 deletion	0.55	549	89.32	384
a/Δ sfl2 deletion	0.35	566	< 0.26[a]	389
a/Δ ume6 deletion	< 0.15	661	79.25	535
a/Δ brg1 sfl2 double deletion	< 0.20	505	100.00	430
a/Δ brg1 ume6 double deletion	< 0.19	539	97.67	730
a/Δ sfl2 ume6 double deletion	0.22	450	100.00	522
a/Δ brg1 sfl2 ume6 triple deletion	0.72	557	100.00	572
a/Δ brg1 sfl2 ume6 rfx2 quad deletion	4.34	392	100.00	371
a/Δ sfl2 brg1 rfx2 ume6 quad deletion	0.26	760	100.00	858
a/Δ ume6 rfx2 brg1 sfl2 quad deletion	0.36	842	100.00	801
a/Δ rfx2 ume6 sfl2 brg1 quad deletion	< 0.09	1060	100.00	1123

Data for additional deletion strains and conditions are presented in Supplementary File 4.
[a] Due to extreme filamentation, hard to score cell type.

Broadly speaking, the results so far indicate that, in SC5314 cells, the conditions that induce white-to-opaque switching are also those reported to strongly induce filamentation in wild-type SC5314. Several previous studies have posited some form of antagonism between the induction of white–opaque switching and filamentation; for example, acidic pH results in increased white-to-opaque switching and decreased filamentation, while neutral or alkaline pH results in decreased white-to-opaque switching and increased filamentation (Sun *et al.* 2015). We previously reported that 2 deletion strains reported to exhibit increased filamentation (*hsl1* and *ssn3*) do not appear to form opaque cells (Brenes *et al.* 2020). It has also been observed that signals which normally favor 1 of these programs can favor the second in cases where the first program is not accessible for some reason. Specifically, it has been reported that ectopic overexpression of the transcriptional regulator Ofi1, which normally results in increased white-to-opaque switching, can lead to filamentation when the opaque cell type is not accessible due to deletion of *WOR1* (Du *et al.* 2015). These results from the literature, in combination with our new results, led to the hypothesis that an abnormally high filamentation response to GlcNAc and CO_2 in SC5314 blocks white-to-opaque switching in a/α cells; however, these same signals give rise to opaque cells in other a/α strains or in SC5314 if the filamentation response is blocked by mutation. A prediction of this hypothesis is that these same mutations would also boost white–opaque switching in SC5314 **a** and α cells, as this same antagonism between switching and filamentation is also predicted to exist in this context. To test this hypothesis, we converted a subset of the single and combination transcription regulator deletion strains in SC5314 a/α to the **a** cell type and measured white-to-opaque switching rates on combinations of glucose, GlcNAc, ambient air, and CO_2. Consistent with our previous report (Lohse *et al.* 2016), none of the single deletions tested had large effects on switching on glucose in ambient air (Table 2; Supplementary File 4). However, the *brg1* and *ume6* single deletions (as well as the combination deletions) had significantly increased switching rates on GlcNAc and CO_2, ranging from 80% (single deletions) to 100% of colonies scored (double, triple, and quadruple deletions) (Table 2; Supplementary File 4).

As with the a/α deletion strains, the results with **a** cells demonstrate that both GlcNAc and CO_2 are needed for maximal switching rates. These results show, consistent with the hypothesis, that the predisposition to filamentation prevents (in the case of a/α cells) or significantly reduces (in the case of **a** cells) the frequency of white-to-opaque switching in the SC5314 background.

Why do other a/α strains form or not form opaque cells?

Our transcriptional profiling indicates that, in the presence of GlcNAc and CO_2, SC5314 is an outlier relative to the other a/α strains examined in this study. The unique response of SC5314 to these 2 signals explains why SC5314 a/α cells do not undergo white–opaque switching. This explanation does not, however, explain why some of the other a/α strains examined here do not readily undergo white–opaque switching. Although not an initial goal of this study, our results do provide additional information regarding this question. We profiled white–opaque switching rates in 26 a/α strains (16 switching-capable and 10 apparently switching-incapable) to better understand the behavior of these strains and search for differences among them that might help to explain their different abilities to undergo white–opaque switching.

Based on the results of these analyses, we reached 5 main conclusions. First, when switched to **a** or α mating types, all 26 strains could form opaque cells (Fig. 3a; Supplementary File 5). In other words, the white–opaque switching apparatus is intact in all strains examined. Second, the switching rates in **a** or α cells relative to their a/α cell parents was routinely higher, indicating that a1/α2 repression of switching still functions in both switching and nonswitching strains, although it is not sufficient to completely block switching (Fig. 3b; Supplementary File 5). Third, the increase in switching rates in the presence of GlcNAc (relative to glucose) and CO_2 (relative to air) indicates that both these signals broadly stimulate white-to-opaque switching in the isolates examined (Fig. 3c and d; Supplementary File 5). Fourth, the magnitudes of a1/α2 repression, GlcNAc stimulation, and CO_2 stimulation effects on switching vary across isolates. Finally, **a** or α cells derived from a/α switching-capable strains tend to have higher white-to-opaque switching rates than those derived from a/α switching-incapable strains ($P = 0.018$, Welch's *t*-test, 2-tailed) (Fig. 3e; Supplementary File 5). Thus, the apparent inability to form opaque cells observed for 10 a/α strains reflects strain-dependent differences in the regulation of switching; the switching apparatus itself is intact in all strains examined.

We also examined opaque cell stability for these strains (that is, opaque-to-white switching), and the results can be summarized by 4 main observations. First, a/α, **a**, and α opaque cells are more stable on GlcNAc than glucose, and this effect is most apparent in a/α cells (Fig. 4a and b; Supplementary File 5). Second, a/α opaque cells are less stable than **a** or α opaque cells derived from the same strain suggesting that a1/α2 repression reduces opaque cell stability in a/α strains (Fig. 4c and d; Supplementary File 5). Third, many a/α strains form opaque cells that are stable in the absence of CO_2, suggesting that CO_2 is more important for the establishment than the maintenance of the opaque cell type. Finally, **a** or α opaque cells derived from a/α switching-incapable strains tend to be less stable than those derived from a/α switching-capable strains (Fig. 4e and f; Supplementary File 5).

As described above, the non-SC5314 a/α strains we have examined display a range of switching frequencies including some that have not been observed to switch. One hypothesis to explain these differences is that they differ in expression of Wor1, the "master" transcriptional regulator of the opaque state. To test this idea, we monitored *WOR1* mRNA levels across 16 of the clinical strains and found a trend: switching-capable strains had higher levels of *WOR1* mRNA than the nonswitching strains. Relative to the level of *WOR1* in SC5314 a/α cells, *WOR1* mRNA levels were ~15% higher in the switching-capable strains and 25% lower in switching-incapable strains (Fig. 3f; Supplementary File 2). There are 3 outliers that do not fit this trend (1 switching, 2 nonswitching), and the results, taken as a single data set, are not statistically significant ($P = 0.0043$ for the *WOR1* ORF; $P = 0.05$ threshold with correction for multiple testing is $P = 0.0007$). However, it is possible that the 3 outliers have a different underlying mechanism for regulating white–opaque switching and that subtle differences in *WOR1* expression can at least partially explain the differing abilities of a/α strains to undergo white–opaque switching. Consistent with this hypothesis, experiments in the literature have shown that subtle changes in *WOR1* expression and/or function (e.g. deletion of 1 of the 2 endogenous copies, fusing GFP to the Wor1 protein) affect both white-to-opaque and opaque-to-white switching rates (Lohse and Johnson 2010; Ziv *et al.* 2022).

Discussion

In this paper, we uncover the basis for an important difference between the standard reference strain of *C. albicans* (SC5314) and a range of other clinical isolates. Based on work in SC5314, white–opaque switching—the formation of 2 heritable cell types from the same genome—was observed in **a** or α strains but not in a/α strains. This difference was due to a block imposed by the MTLa1/MTLα2 heterodimer repressor, which only forms in a/α cells. However, subsequent work showed that, in many other clinical isolates of *C. albicans*, a/α cells could undergo white–opaque switching. In this paper, we resolve this apparent paradox; our principle conclusions are as follows:

(1) The SC5314 a/α reference strain differs from the other *C. albicans* a/α strains examined here by highly inducing 4 filamentation-associated transcriptional regulators (BRG1, SFL2, UME6, and RFX2) in response to GlcNAc and CO2. This induction, which was not observed or was observed to a lesser extent in the other clinical strains, blocks white–opaque switching in SC5314 a/α cells. When all 4 genes are deleted, SC5314 can now readily undergo white–opaque switching as an a/α strain; in other words, there are 2 regulatory blocks to white-to-opaque switching in SC5314 a/α cells that operate independently: (1) MTLa1/MTLα2 repression of WOR1 expression and (2) upregulation of BRG1, SFL2, UME6, and RFX2 in response to GlcNAc and CO2 (Fig. 5). When a single block is removed, either by converting SC5314 a/α to a or α cells or by deleting BRG1 and SFL2, white-to-opaque switching can readily occur. When both blocks are removed simultaneously, switching rates become even higher, approaching 100%.

We further show that, in the 26 non-SC5314 clinical strains examined here, the MTLa1/MTLα2 regulatory block is intact, but the second block is missing. This allows many of these strains to undergo white–opaque switching as a/α strains. When the first block (repression by the MTLa1/MTLα2 heterodimer) is also removed, these strains undergo switching at even higher rates and even the "nonswitching" strains become switching competent.

(2) Maximum switching rates for SC5314 a/α strains are observed when combinations of brg1, sfl2, ume6, and rfx2 knockouts are tested, indicating that multiple genomic loci underlie the difference in the regulation of white–opaque switching between SC5314 and the other clinical isolates.

(3) Our results, in combination with published results, suggest that an antagonism exists between filamentous growth and white-to-opaque switching and the "set point" of this

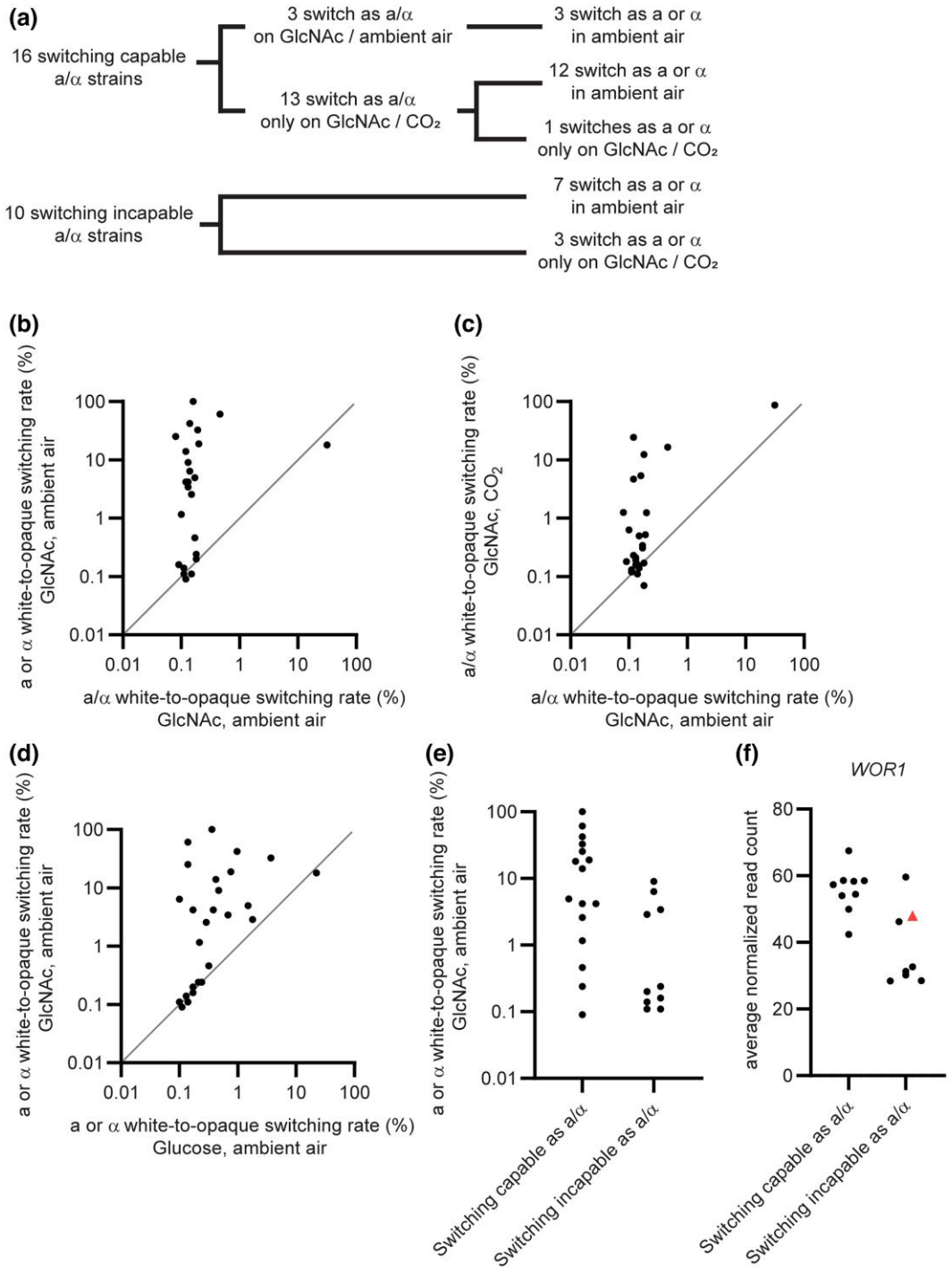

Fig. 3. White-to-opaque switching frequencies of 26 non-SC5314 clinical strains in response to mating type, carbon source, and atmospheric differences. a) Summary of the switching phenotypes observed for 26 a/α clinical strains and the a or α strains derived from them. b) White-to-opaque switching frequencies of 25 a/α strains (x-axis) and the a or α strains derived from them (y-axis) on GlcNAc in ambient air. c) White-to-opaque switching frequencies of 16 switching-capable a/α strains on GlcNAc when exposed to ambient air (x-axis) or CO_2 (y-axis). d) White-to-opaque switching frequencies of 26 a or α strains, derived from a/α strains, growing on glucose (x-axis) or GlcNAc (y-axis) in ambient air. e) White-to-opaque switching frequencies of 26 a or α strains derived from 16 switching-capable (left) or 10 switching-incapable (right) a/α strains when grown on GlcNAc in ambient air. f) Normalized read counts for *WOR1* in 9 switching-capable and 8 switching-incapable (including SC5314) a/α strains. Non-SC5314 strains are indicated with black circles; SC5314 is indicated with a red triangle. Each point represents the average of all replicates for a given strain (4 for SC5314, 2 for all other strains). In b–e, axes are plotted on a log10 scale, and when no switching events were detected for a strain in an assay, the switching rate is reported as 100 divided by the total number of colonies counted for that strain in the assay. In b–d, the line of identity ($y = x$) is indicated.

antagonism differs between SC5314 and the other clinical strains. As discussed above, changes in the environment and many genetic manipulations can affect white–opaque switching (Du *et al.* 2015; Sun *et al.* 2015; Ene *et al.* 2016; Lohse *et al.* 2016; Brenes *et al.* 2020). The work described in this paper strongly suggests that the balance between filamentous growth and white–opaque switching is also shifted by naturally occurring strain variation.

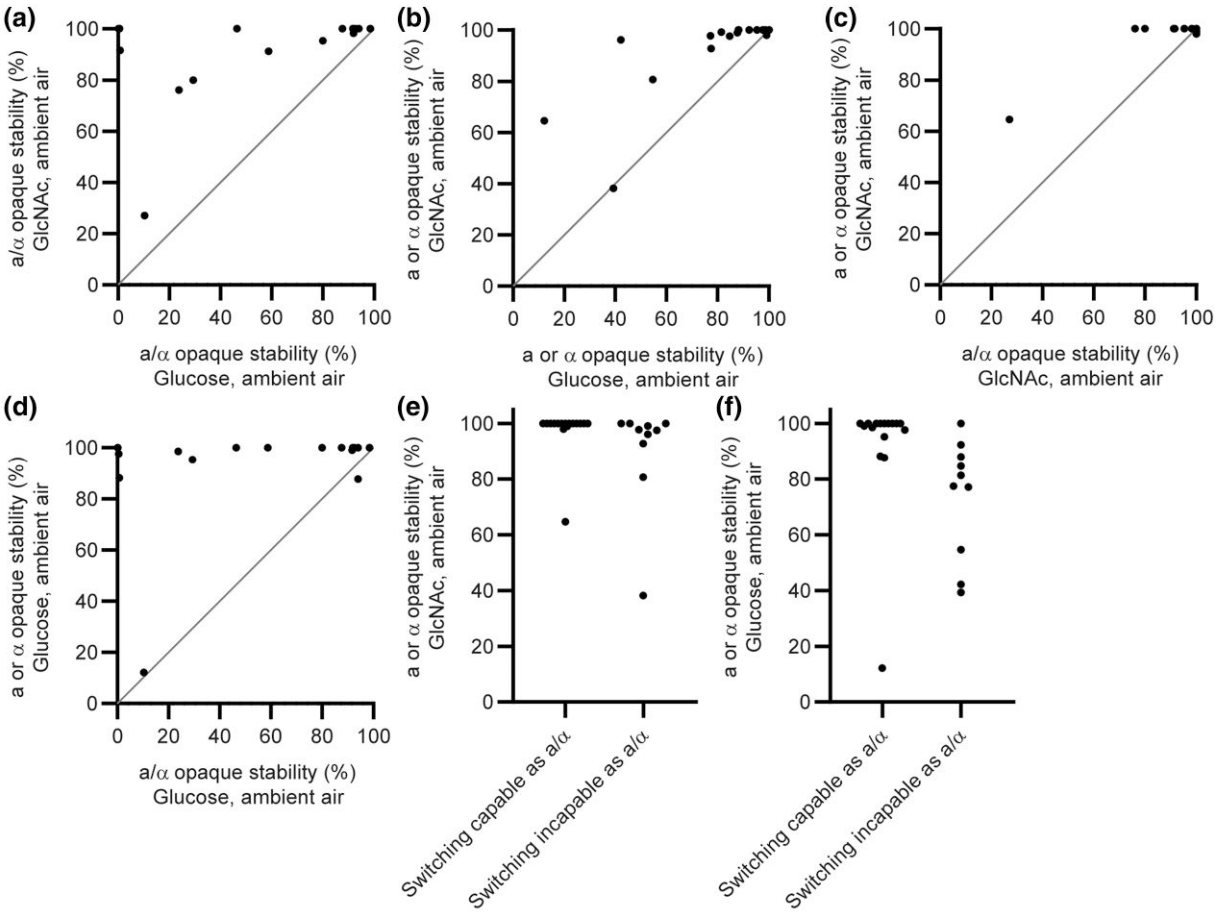

Fig. 4. Opaque stability of 26 non-SC5314 strains in response to mating type, carbon source, and atmospheric differences. a) Opaque stability of 16 a/α strains growing on glucose (x-axis) or GlcNAc (y-axis) in ambient air. b) Opaque stability of 26 a or α strains, derived from a/α strains, growing on glucose (x-axis) or GlcNAc (y-axis) in ambient air. c) Opaque stability of 16 a/α strains (x-axis) and the a or α strains derived from them (y-axis) on GlcNAc in ambient air. d) Opaque stability of 16 a/α strains (x-axis) and the a or α strains derived from them (y-axis) on glucose in ambient air. e) Opaque stability of 26 a or α strains derived from 16 switching-capable (left) or 10 switching-incapable (right) a/α strains when grown on GlcNAc in ambient air. f) Opaque stability of 26 a or α strains derived from 16 switching-capable (left) or 10 switching-incapable (right) a/α strains when grown on glucose in ambient air. In all panels, when no opaque cells were detected for a strain in an assay, the opaque stability is reported as 100 divided by the total number of colonies counted for that strain in the assay. In a–d, the line of identity ($y = x$) is indicated.

(4) Although not a primary goal of this work, we did notice a trend in the non-SC5314 clinical strains between expression of WOR1 mRNA and the ability to undergo white–opaque switching as an a/α strain. This trend was not observed for all strains (there were 3 outliers), but it suggests that subtle differences in WOR1 expression could explain some of the differences among the non-SC5314 clinical strains.
(5) For the 26 non-SC5314 strains, we showed that all of them (both switching competent and nonswitchers) have the ability to undergo white-to-opaque switching when converted to a or α cells. Thus, the switching apparatus is intact in all of these strains, and the difference in switching rates in a/α cells reflects regulation of white–opaque switching rather than its inactivation. It is possible that the "nonswitching" a/α strains are capable of switching under environmental conditions that have not yet been investigated.

In conclusion, we show that there are 2 potential blocks to white–opaque switching: (1) the well-studied block of the MTLa1/MTLα2 repressor present only in a/α cells and (2) the induction of a series of transcriptional regulators (*BRG1*, *SFL2*, *UME6*, and *RFX2*) that is independent of MTLa1/MTLα2 repression. The reference strain (SC5314) contains both blocks, thereby preventing white–opaque switching unless at least 1 of the blocks is removed, either through genetic manipulation or through naturally occurring strain variation. In the 16 additional clinical strains investigated here, the first block was present, but the second block was absent. This absence allowed many of these strains to undergo white–opaque switching even when they are a/α cells and therefore contain the first block. We also show that, for those non-SC5314 strains that have not been observed to undergo white–opaque switching, if the a/α block is removed (by converting them to **a** or α cells), they now become switching competent. These results show that the white–opaque switching apparatus is intact across a wide variety of strains and that it is the regulation of switching (rather than its presence or absence) that differs among clinical isolates. Many different environmental signals converge to regulate the rate of white–opaque switching, and not surprisingly many different genes also affect the rate (Ene *et al.* 2016; Lohse *et al.* 2016; Brenes *et al.* 2020). White–opaque switching is widely conserved among clinical strains and extends to *Candida dubliniensis* and *Candida tropicalis* (Pujol *et al.* 2004; Porman *et al.* 2011), indicating that it is under strong selection and must be of key importance for those species that maintain

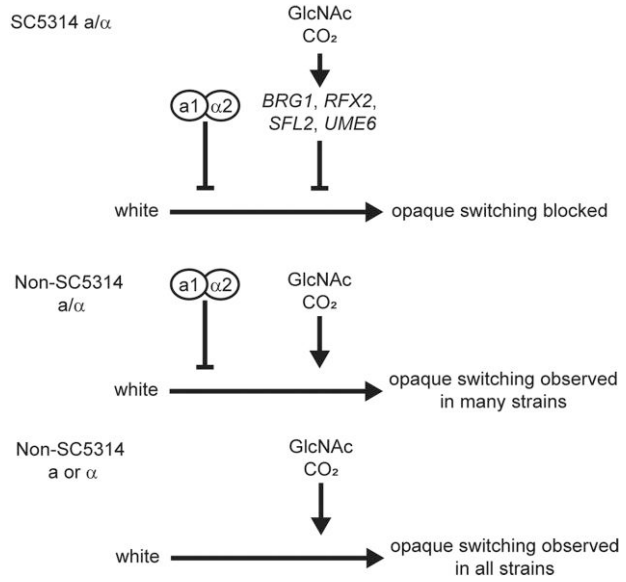

Fig. 5. Model for regulation of white-to-opaque switching in *C. albicans*. In SC5314 a/α (top), there are 2 blocks to white–opaque switching, the MTLa1/MTLα2 heterodimer, and the induction of *BRG1*, *SFL2*, *UME6*, and *RFX2* by GlcNAc and CO_2. As described in the text, if either block is removed, white-to-opaque switching occurs at low rates; if both blocks are removed, switching occurs at very high levels. In the a/α non-SC5314 strains studied here, the induction of *BRG1*, *SFL2*, *UME6*, and *RFX2* by GlcNAc and CO_2 does not occur to the same extent (if at all), and strains can undergo switching (middle). If the MTLa1/MTLα2 block is removed (that is, if the strains are converted to a or α strains), switching rates increase (bottom). Even those strains not observed to switch as a/α cells undergo opaque switching when converted to a cells.

it. The work in this paper, combined with previous work, shows that, although the regulation of white–opaque switching differs across *C. albicans* clinical strains, the underlying process itself remains intact.

Data availability

Strains and plasmids are available upon request. The authors affirm that all data necessary for confirming the conclusions of the article are present within the article, figures, tables, supplemental figures, and supplemental files. Supplementary File 1 contains lists of the oligonucleotides, plasmids, and strains used in this study. Supplementary File 2 contains the compiled data and information for the NanoString experiments from this study. The raw and normalized NanoString data are also available as accession number GSE241766 at the NCBI Gene Expression Omnibus (GEO). Supplementary Files 3–5 contain the data for the switching assays related to this study.

Supplemental material available at GENETICS online.

Acknowledgments

We thank members of the Johnson Lab, especially Lucas Brenes, Carrie Graham, Chien-Der Lee, and Harold Marin, for helpful discussions and suggestions. We thank Ananda Mendoza for technical support. We thank the Laboratory for Cell Analysis—Genome Core Facility at UCSF and especially Emanuela Zacco, for help with the NanoString experiments. We thank Iuliana Ene for Bioinformatics support.

Funding

This work was supported by National Institutes of Health (NIH) grants R01AI049187 and R01GM037049 (to A.D.J.). This study was also supported in part by the Helen Diller Family Comprehensive Cancer Center Laboratory for Cell Analysis Shared Resource Facility through a grant from the NIH (P30CA082103). The content is the sole responsibility of the authors and does not represent the views of the NIH or other funding agencies. Neither the NIH nor other funding agencies had any role in the design of the study, in the collection, analyses, or interpretation of data, in the writing of the manuscript, or in the decision to publish the results.

Conflicts of interest

ADJ is a cofounder of BioSynesis, Inc., a company developing diagnostics and therapeutics for biofilm infections. MBL is a consultant for BioSynesis, Inc. No funding for this research was provided by BioSynesis, Inc. and/or by any grants to BioSynesis, Inc. Neither BioSynesis, Inc., nor agencies funding BioSynesis, Inc., played any role in the study design, data collection and analysis, decision to publish, or preparation of the manuscript.

Literature cited

Achkar JM, Fries BC. 2010. *Candida* infections of the genitourinary tract. Clin Microbiol Rev. 23(2):253–273. doi:10.1128/CMR.00076-09.

Aszalos A, Robison RS, Lemanski P, Berk B. 1968. Trienine, an antitumor triene antibiotic. J Antibiot (Tokyo). 21(10):611–615. doi:10.7164/antibiotics.21.611.

Banerjee M, Thompson DS, Lazzell A, Carlisle PL, Pierce C, Monteagudo C, López-Ribot JL, Kadosh D. 2008. *UME6*, a novel filament-specific regulator of *Candida albicans* hyphal extension and virulence. Mol Biol Cell. 19(4):1354–1365. doi:10.1091/mbc.e07-11-1110.

Beekman CN, Cuomo CA, Bennett RJ, Ene IV. 2021. Comparative genomics of white and opaque cell states supports an epigenetic mechanism of phenotypic switching in *Candida albicans*. G3 (Bethesda). 11(2):jkab001. doi:10.1093/g3journal/jkab001.

Bergen MS, Voss E, Soll DR. 1990. Switching at the cellular level in the white–opaque transition of *Candida albicans*. J Gen Microbiol. 136(10):1925–1936. doi:10.1099/00221287-136-10-1925.

Blignaut E, Pujol C, Lockhart S, Joly S, Soll DR. 2002. Ca3 fingerprinting of *Candida albicans* isolates from human immunodeficiency virus-positive and healthy individuals reveals a new clade in South Africa. J Clin Microbiol. 40(3):826–836. doi:10.1128/JCM.40.3.826-836.2002.

Brenes LR, Lohse MB, Hartooni N, Johnson AD. 2020. A set of diverse genes influence the frequency of white–opaque switching in *Candida albicans*. G3 (Bethesda). 10(8):2593–2600. doi:10.1534/g3.120.401249.

Calderone RA, Fonzi WA. 2001. Virulence factors of *Candida albicans*. Trends Microbiol. 9(7):327–335. doi:10.1016/S0966-842X(01)02094-7.

Cao C, Wu M, Bing J, Tao L, Ding X, Liu X, Huang G. 2017. Global regulatory roles of the cAMP/PKA pathway revealed by phenotypic, transcriptomic and phosphoproteomic analyses in a null mutant of the PKA catalytic subunit in *Candida albicans*. Mol Microbiol. 105(1):46–64. doi:10.1111/mmi.13681.

Carlisle PL, Banerjee M, Lazzell A, Monteagudo C, López-Ribot JL, Kadosh D. 2009. Expression levels of a filament-specific

transcriptional regulator are sufficient to determine *Candida albicans* morphology and virulence. Proc Natl Acad Sci U S A. 106(2): 599–604. doi:10.1073/pnas.0804061106.

Cleary IA, Lazzell AL, Monteagudo C, Thomas DP, Saville SP. 2012. *BRG1* And *NRG1* form a novel feedback circuit regulating *Candida albicans* hypha formation and virulence. Mol Microbiol. 85(3):557–573. doi:10.1111/j.1365-2958.2012.08127.x.

Correia I, Wilson D, Hube B, Pla J. 2020. Characterization of a *Candida albicans* mutant defective in all MAPKs highlights the major role of Hog1 in the MAPK signaling network. J. Fungi (Basel). 6(4): 230. doi:10.3390/jof6040230.

Deng F-S, Lin C-H. 2018. Cpp1 phosphatase mediated signaling cross-talk between Hog1 and Cek1 mitogen-activated protein kinases is involved in the phenotypic transition in *Candida albicans*. Med Mycol. 56(2):242–252. doi:10.1093/mmy/myx027.

Ding X, Cao C, Zheng Q, Huang G. 2017. The regulatory subunit of protein kinase A (bcy1) in *Candida albicans* plays critical roles in filamentation and white–opaque switching but is not essential for cell growth. Front Microbiol. 7:2127. doi:10.3389/fmicb.2016.02127.

Du H, Li X, Huang G, Kang Y, Zhu L. 2015. The zinc-finger transcription factor, Ofi1, regulates white–opaque switching and filamentation in the yeast *Candida albicans*. Acta Biochim Biophys Sin (Shanghai). 47(5):335–341. doi:10.1093/abbs/gmv011.

Dumitru R, Navarathna DH, Semighini CP, Elowsky CG, Dumitru RV, Dignard D, Whiteway M, Atkin AL, Nickerson KW. 2007. *In vivo* and *in vitro* anaerobic mating in *Candida albicans*. Eukaryot Cell. 6(3):465–472. doi:10.1128/EC.00316-06.

Eggimann P, Garbino J, Pittet D. 2003. Epidemiology of *Candida* species infections in critically ill non-immunosuppressed patients. Lancet Infect Dis. 3(11):685–702. doi:10.1016/S1473-3099(03)00801-6.

Ellis B, Haaland P, Hahne F, Le Meur N, Gopalakrishnan N, Spidlen J, Jiang M, Finak G. 2019. flowCore: Basic structures for flow cytometry data. R package version 1.50.0.

Ene IV, Lohse MB, Vladu AV, Morschhäuser J, Johnson AD, Bennett RJ. 2016. Phenotypic profiling reveals that *Candida albicans* opaque cells represent a metabolically specialized cell state compared to default white cells. mBio. 7(6):e01269-16. doi:10.1128/mBio.01269-16.

Fox EP, Cowley ES, Nobile CJ, Hartooni N, Newman DK, Johnson AD. 2014. Anaerobic bacteria grow within *Candida albicans* biofilms and induce biofilm formation in suspension cultures. Curr Biol. 24(20):2411–2416. doi:10.1016/j.cub.2014.08.057.

Geiger J, Wessels D, Lockhart SR, Soll DR. 2004. Release of a potent polymorphonuclear leukocyte chemoattractant is regulated by white–opaque switching in *Candida albicans*. Infect Immun. 72(2):667–677. doi:10.1128/IAI.72.2.667-677.2004.

Gudlaugsson O, Gillespie S, Lee K, Vande Berg J, Hu J, Messer S, Herwaldt L, Pfaller M, Diekema D. 2003. Attributable mortality of nosocomial candidemia, revisited. Clin Infect Dis. 37(9): 1172–1177. doi:10.1086/378745.

Hao B, Clancy CJ, Cheng S, Raman SB, Iczkowski KA, Nguyen MH. 2009. *Candida albicans RFX2* encodes a DNA binding protein involved in DNA damage responses, morphogenesis, and virulence. Eukaryot Cell. 8(4):627–639. doi:10.1128/EC.00246-08.

Hernday AD, Lohse MB, Fordyce PM, Nobile CJ, DeRisi JD, Johnson AD. 2013. Structure of the transcriptional network controlling white–opaque switching in *Candida albicans*. Mol Microbiol. 90(1):22–35. doi:10.1111/mmi.12329.

Hernday AD, Lohse MB, Nobile CJ, Noiman L, Laksana CN, Johnson AD. 2016. Ssn6 defines a new level of regulation of white–opaque switching in *Candida albicans* and is required for the stochasticity of the switch. mBio. 7(1):e01565-15. doi:10.1128/mBio.01565-15.

Hernday AD, Noble SM, Mitrovich QM, Johnson AD. 2010. Genetics and molecular biology in *Candida albicans*. Methods Enzymol. 470:737–758. doi:10.1016/S0076-6879(10)70031-8.

Hirakawa MP, Martinez DA, Sakthikumar S, Anderson MZ, Berlin A, Gujja S, Zeng Q, Zisson E, Wang JM, Greenberg JM, *et al.* 2015. Genetic and phenotypic intra-species variation in *Candida albicans*. Genome Res. 25(3):413–425. doi:10.1101/gr.174623.114.

Homann OR, Dea J, Noble SM, Johnson AD. 2009. A phenotypic profile of the *Candida albicans* regulatory network. PLoS Genet. 5(12): e1000783. doi:10.1371/journal.pgen.1000783.

Hornby JM, Jensen EC, Lisec AD, Tasto JJ, Jahnke B, Shoemaker R, Dussault P, Nickerson KW. 2001. Quorum sensing in the dimorphic fungus *Candida albicans* is mediated by farnesol. Appl Environ Microbiol. 67(7):2982–2992. doi:10.1128/AEM.67.7.2982-2992.2001.

Hu J, Guan G, Dai Y, Tao L, Zhang J, Li H, Huang G. 2016. Phenotypic diversity and correlation between white–opaque switching and the CAI microsatellite locus in *Candida albicans*. Curr Genet. 62(3):585–593. doi:10.1007/s00294-016-0564-8.

Huang MY, Cravener MC, Mitchell AP. 2021. Targeted genetic changes in *Candida albicans* using transient CRISPR-Cas9 expression. Curr Protoc. 1(1):e19. doi:10.1002/cpz1.19.

Huang G, Wang H, Chou S, Nie X, Chen J, Liu H. 2006. Bistable expression of *WOR1*, a master regulator of white–opaque switching in *Candida albicans*. Proc Natl Acad Sci USA. 103(34):12813–12818. doi:10.1073/pnas.0605270103.

Huang G, Yi S, Sahni N, Daniels KJ, Srikantha T, Soll DR. 2010. N-acetylglucosamine induces white to opaque switching, a mating prerequisite in *Candida albicans*. PLoS Pathog. 6(3):e1000806. doi:10.1371/journal.ppat.1000806.

Hull CM, Johnson AD. 1999. Identification of a mating type-like locus in the asexual pathogenic yeast *Candida albicans*. Science. 285(5431):1271–1275. doi:10.1126/science.285.5431.1271.

Hull CM, Raisner RM, Johnson AD. 2000. Evidence for mating of the "asexual" yeast *Candida albicans* in a mammalian host. Science. 289(5477):307–310. doi:10.1126/science.289.5477.307.

Johnson A. 2003. The biology of mating in *Candida albicans*. Nat Rev Microbiol. 1(2):106–116. doi:10.1038/nrmicro752.

Kennedy MJ, Volz PA. 1985. Ecology of *Candida albicans* gut colonization: inhibition of *Candida* adhesion, colonization, and dissemination from the gastrointestinal tract by bacterial antagonism. Infect Immun. 49(3):654–663. doi:10.1128/iai.49.3.654-663.1985.

Kim J, Sudbery P. 2011. *Candida albicans*, a major human fungal pathogen. J Microbiol. 49(2):171–177. doi:10.1007/s12275-011-1064-7.

Kullberg BJ, Oude Lashof AML. 2002. Epidemiology of opportunistic invasive mycoses. Eur J Med Res. 7(5):183–191.

Kumamoto CA. 2011. Inflammation and gastrointestinal *Candida* colonization. Curr Opin Microbiol. 14(4):386–391. doi:10.1016/j.mib.2011.07.015.

Kvaal C, Lachke SA, Srikantha T, Daniels K, McCoy J, Soll DR. 1999. Misexpression of the opaque-phase-specific gene *PEP1* (*SAP1*) in the white phase of *Candida albicans* confers increased virulence in a mouse model of cutaneous infection. Infect Immun. 67(12): 6652–6662. doi:10.1128/IAI.67.12.6652-6662.1999.

Kvaal CA, Srikantha T, Soll DR. 1997. Misexpression of the white-phase-specific gene *WH11* in the opaque phase of *Candida albicans* affects switching and virulence. Infect Immun. 65(11): 4468–4475. doi:10.1128/iai.65.11.4468-4475.1997.

Lan C, Newport G, Murillo L, Jones T, Scherer S, Davis RW, Agabian N. 2002. Metabolic specialization associated with phenotypic switching in *Candida albicans*. Proc Natl Acad Sci USA. 99(23): 14907–14912. doi:10.1073/pnas.232566499.

Li H-M, Shimizu-Imanishi Y, Tanaka R, Li R-Y, Yaguchi T. 2016. White–opaque switching in different mating type-like locus gene types of clinical *Candida albicans* isolates. Chin Med J. 129(22):2725–2732. doi:10.4103/0366-6999.193442.

Liang SH, Cheng JH, Deng FS, Tsai PA, Lin CH. 2014. A novel function for Hog1 stress-activated protein kinase in controlling white–opaque switching and mating in *Candida albicans*. Eukaryot Cell. 13(12):1557–1566. doi:10.1128/EC.00235-14.

Lin CH, Kabrawala S, Fox EP, Nobile CJ, Johnson AD, Bennett RJ. 2013. Genetic control of conventional and pheromone-stimulated biofilm formation in *Candida albicans*. PLoS Pathog. 9(4):e1003305. doi:10.1371/journal.ppat.1003305.

Lockhart SR, Pujol C, Daniels KJ, Miller MG, Johnson AD, Pfaller MA, Soll DR. 2002. In *Candida albicans*, white–opaque switchers are homozygous for mating type. Genetics. 162(2):737–745. doi:10.1093/genetics/162.2.737.

Lockhart SR, Reed BD, Pierson CL, Soll DR. 1996. Most frequent scenario for recurrent *Candida* vaginitis is strain maintenance with "substrain shuffling": demonstration by sequential DNA fingerprinting with probes Ca3, C1, and CARE2. J Clin Microbiol. 34(4):767–777. doi:10.1128/jcm.34.4.767-777.1996.

Lohse MB, Brenes LR, Ziv N, Winter MB, Craik CS, Johnson AD. 2020. An opaque cell-specific expression program of secreted proteases and transporters allows cell-type cooperation in *Candida albicans*. Genetics. 216(2):409–429. doi:10.1534/genetics.120.303613.

Lohse MB, Ene IV, Craik VB, Hernday AD, Mancera E, Morschhäuser J, Bennett RJ, Johnson AD. 2016. Systematic genetic screen for transcriptional regulators of the *Candida albicans* white–opaque switch. Genetics. 203(4):1679–1692. doi:10.1534/genetics.116.190645.

Lohse MB, Hernday AD, Fordyce PM, Noiman L, Sorrells TR, Hanson-Smith V, Nobile CJ, DeRisi JL, Johnson AD. 2013. Identification and characterization of a previously undescribed family of sequence-specific DNA-binding domains. Proc Natl Acad Sci USA. 110(19):7660–7665. doi:10.1073/pnas.1221734110.

Lohse MB, Johnson AD. 2008. Differential phagocytosis of white versus opaque *Candida albicans* by *Drosophila* and mouse phagocytes. PLoS One. 3(1):e1473. doi:10.1371/journal.pone.0001473.

Lohse MB, Johnson AD. 2009. White–opaque switching in *Candida albicans*. Curr Opin Microbiol. 12(6):650–654. doi:10.1016/j.mib.2009.09.010.

Lohse MB, Johnson AD. 2010. Temporal anatomy of an epigenetic switch in cell programming: the white–opaque transition of *C. albicans*. Mol Microbiol. 78(2):331–343. doi:10.1111/j.1365-2958.2010.07331.x.

Lohse MB, Johnson AD. 2016. Identification and characterization of Wor4, a new transcriptional regulator of white–opaque switching. G3 (Bethesda). 6(3):721–729. doi:10.1534/g3.115.024885.

Lu Y, Su C, Ray S, Yuan Y, Liu H. 2019. CO2 Signaling through the Ptc2-Ssn3 axis governs sustained hyphal development of *Candida albicans* by reducing ume6 phosphorylation and degradation. MBio. 10(1):e02320-18. doi:10.1128/mBio.02320-18.

Lu Y, Su C, Solis NV, Filler SG, Liu H. 2013. Synergistic regulation of hyphal elongation by hypoxia, CO(2), and nutrient conditions controls the virulence of *Candida albicans*. Cell Host Microbe. 14(5):499–509. doi:10.1016/j.chom.2013.10.008.

Maestrone G, Semar R. 1968. Establishment and treatment of cutaneous *Candida albicans* infection in the rabbit. Naturwissenschaften. 55(2):87–88. doi:10.1007/BF00599501.

Magee BB, Magee PT. 2000. Induction of mating in *Candida albicans* by construction of MTLa and MTLalpha strains. Science. 289(5477):310–313. doi:10.1126/science.289.5477.310.

Mendelsohn S, Pinsky M, Weissman Z, Kornitzer D. 2017. Regulation of the *Candida albicans* hypha-inducing transcription factor Ume6 by the *CDK1* cyclins Cln3 and Hgc1. mSphere. 2(2):e00248-16. doi:10.1128/mSphere.00248-16.

Meyers E, Miragila GJ, Smith DA, Basch HI, Pansy FE, Trejo WH, Donovick R. 1968. Biological characterization of prasinomycin, a phosphorus-containing antibiotic. Appl Microbiol. 16(4):603–608. doi:10.1128/am.16.4.603-608.1968.

Miller MG, Johnson AD. 2002. White–opaque switching in *Candida albicans* is controlled by mating-type locus homeodomain proteins and allows efficient mating. Cell. 110(3):293–302. doi:10.1016/S0092-8674(02)00837-1.

Morschhäuser J. 2010. Regulation of white–opaque switching in *Candida albicans*. Med Microbiol Immunol. 199(3):165–172. doi:10.1007/s00430-010-0147-0.

Naseem S, Gunasekera A, Araya E, Konopka JB. 2011. N-Acetylglucosamine (GlcNAc) induction of hyphal morphogenesis and transcriptional responses in *Candida albicans* are not dependent on its metabolism. J Biol Chem. 286(33):28671–28680. doi:10.1074/jbc.M111.249854.

Nguyen N, Quail MMF, Hernday AD. 2017. An efficient, rapid, and recyclable system for CRISPR-mediated genome editing in *Candida albicans*. mSphere. 2(2):e00149-17. doi:10.1128/mSphereDirect.00149-17.

Noble SM, Johnson AD. 2005. Strains and strategies for large-scale gene deletion studies of the diploid human fungal pathogen *Candida albicans*. Eukaryot Cell. 4(2):298–309. doi:10.1128/EC.4.2.298-309.2005.

Odds FC, Bougnoux ME, Shaw DJ, Bain JM, Davidson AD, Diogo D, Jacobsen MD, Lecomte M, Li S-Y, Tavanti A, *et al.* 2007. Molecular phylogenetics of *Candida albicans*. Eukaryot Cell. 6(6):1041–1052. doi:10.1128/EC.00041-07.

Pappas PG, Rex JH, Sobel JD, Filler SG, Dismukes WE, Walsh TJ, Edwards JE. 2004. Guidelines for treatment of candidiasis. Clin Infect Dis. 38(2):161–189. doi:10.1086/380796.

Park Y-N, Conway K, Conway TP, Daniels KJ, Soll DR. 2019. Roles of the transcription factors Sfl2 and Efg1 in white–opaque switching in a/α strains of *Candida albicans*. mSphere. 4(2):e00703-18. doi:10.1128/mSphere.00703-18.

Park Y-N, Conway K, Pujol C, Daniels KJ, Soll DR. 2020. *EFG1* Mutations, phenotypic switching, and colonization by clinical a/α strains of *Candida albicans*. mSphere. 5(1):e00795-19. doi:10.1128/mSphere.00795-19.

Porman AM, Alby K, Hirakawa MP, Bennett RJ. 2011. Discovery of a phenotypic switch regulating sexual mating in the opportunistic fungal pathogen *Candida tropicalis*. Proc Natl Acad Sci USA. 108(52):21158–21163. doi:10.1073/pnas.1112076109.

Pujol C, Daniels KJ, Lockhart SR, Srikantha T, Radke JB, Geiger J, Soll DR. 2004. The closely related species *Candida albicans* and *Candida dubliniensis* can mate. Eukaryot Cell. 3(4):1015–1027. doi:10.1128/EC.3.4.1015-1027.2004.

Pujol C, Pfaller M, Soll DR. 2002. Ca3 fingerprinting of *Candida albicans* bloodstream isolates from the United States, Canada, South America, and Europe reveals a European clade. J Clin Microbiol. 40(8):2729–2740. doi:10.1128/JCM.40.8.2729-2740.2002.

Ramírez-Zavala B, Weyler M, Gildor T, Schmauch C, Kornitzer D, Arkowitz R, Morschhäuser J. 2013. Activation of the Cph1-dependent MAP kinase signaling pathway induces white–opaque switching in *Candida albicans*. PLoS Pathog. 9(10):e1003696. doi:10.1371/journal.ppat.1003696.

R Core Team. 2019. R: A language and environment for statistical computing. R Foundation for Statistical Computing, Vienna, Austria. https://www.R-project.org/.

Rikkerink EH, Magee BB, Magee PT. 1988. Opaque-white phenotype transition: a programmed morphological transition in *Candida*

albicans. J Bacteriol. 170(2):895–899. doi:10.1128/jb.170.2.895-899.1988.

Rodriguez DL, Quail MM, Hernday AD, Nobile CJ. 2020. Transcriptional circuits regulating developmental processes in *Candida albicans*. Front Cell Infect Microbiol. 10:605711. doi:10.3389/fcimb.2020.605711.

Sasse C, Hasenberg M, Weyler M, Gunzer M, Morschhäuser J. 2013. White–opaque switching of *Candida albicans* allows immune evasion in an environment-dependent fashion. Eukaryot Cell. 12(1):50–58. doi:10.1128/EC.00266-12.

Si H, Hernday AD, Hirakawa MP, Johnson AD, Bennett RJ. 2013. *Candida albicans* white and opaque cells undergo distinct programs of filamentous growth. PLoS Pathog. 9(3):e1003210. doi:10.1371/journal.ppat.1003210.

Slutsky B, Staebell M, Anderson J, Risen L, Pfaller M, Soll DR. 1987. "White–opaque transition": a second high-frequency switching system in *Candida albicans*. J Bacteriol. 169(1):189–197. doi:10.1128/jb.169.1.189-197.1987.

Soll DR. 2009. Why does *Candida albicans* switch? FEMS Yeast Res. 9(7):973–989. doi:10.1111/j.1567-1364.2009.00562.x.

Soll DR, Morrow B, Srikantha T. 1993. High-frequency phenotypic switching in *Candida albicans*. Trends Genet. 9(2):61–65. doi:10.1016/0168-9525(93)90189-O.

Song W, Wang H, Chen J. 2011. *Candida albicans* Sfl2, a temperature-induced transcriptional regulator, is required for virulence in a murine gastrointestinal infection model. FEMS Yeast Res. 11(2):209–222. doi:10.1111/j.1567-1364.2010.00710.x.

Sonneborn A, Tebarth B, Ernst JF. 1999. Control of white–opaque phenotypic switching in *Candida albicans* by the Efg1p morphogenetic regulator. Infect Immun. 67(9):4655–4660. doi:10.1128/IAI.67.9.4655-4660.1999.

Spiering MJ, Moran GP, Chauvel M, Maccallum DM, Higgins J, Hokamp K, Yeomans T, d'Enfert C, Coleman DC, Sullivan DJ. 2010. Comparative transcript profiling of *Candida albicans* and *Candida dubliniensis* identifies *SFL2*, a *C. albicans* gene required for virulence in a reconstituted epithelial infection model. Eukaryot Cell. 9(2):251–265. doi:10.1128/EC.00291-09.

Srikantha T, Borneman AR, Daniels KJ, Pujol C, Wu W, Seringhaus MR, Gerstein M, Yi S, Snyder M, Soll DR. 2006. *TOS9* regulates white–opaque switching in *Candida albicans*. Eukaryot Cell. 5(10):1674–1687. doi:10.1128/EC.00252-06.

Srikantha T, Tsai LK, Daniels K, Soll DR. 2000. *EFG1* Null mutants of *Candida albicans* switch but cannot express the complete phenotype of white-phase budding cells. J Bacteriol. 182(6):1580–1591. doi:10.1128/JB.182.6.1580-1591.2000.

Su C, Yu J, Sun Q, Liu Q, Lu Y. 2018. Hyphal induction under the condition without inoculation in *Candida albicans* is triggered by Brg1-mediated removal of *NRG1* inhibition. Mol Microbiol. 108(4):410–423. doi:10.1111/mmi.13944.

Sun Y, Cao C, Jia W, Tao L, Guan G, Huang G. 2015. Ph regulates white–opaque switching and sexual mating in *Candida albicans*. Eukaryot Cell. 14(11):1127–1134. doi:10.1128/EC.00123-15.

Takagi J, Singh-Babak SD, Lohse MB, Dalal CK, Johnson AD. 2019. *Candida albicans* white and opaque cells exhibit distinct spectra of organ colonization in mouse models of infection. PLoS One. 14(6):e0218037. doi:10.1371/journal.pone.0218037.

Tsong AE, Miller MG, Raisner RM, Johnson AD. 2003. Evolution of a combinatorial transcriptional circuit: a case study in yeasts. Cell. 115(4):389–399. doi:10.1016/S0092-8674(03)00885-7.

Tuch BB, Mitrovich QM, Homann OR, Hernday AD, Monighetti CK, De La Vega FM, Johnson AD. 2010. The transcriptomes of two heritable cell types illuminate the circuit governing their differentiation. PLoS Genet. 6(8):e1001070. doi:10.1371/journal.pgen.1001070.

Van P, Jiang W, Gottardo R, Finak G. 2018. Ggcyto: next generation open-source visualization software for cytometry. Bioinformatics. 34(22):3951–3953. doi:10.1093/bioinformatics/bty441.

Vinces M, Kumamoto CA. 2007. The morphogenetic regulator Czf1p is a DNA-binding protein that regulates white opaque switching in *Candida albicans*. Microbiology. 153(9):2877–2884. doi:10.1099/mic.0.2007/005983-0.

Vyas VK, Barrasa MI, Fink GR. 2015. A *Candida albicans* CRISPR system permits genetic engineering of essential genes and gene families. Sci Adv. 1(3):e1500248. doi:10.1126/sciadv.1500248.

Wang H, Song W, Huang G, Zhou Z, Ding Y, Chen J. 2011. *Candida albicans* Zcf37, a zinc finger protein, is required for stabilization of the white state. FEBS Lett. 585(5):797–802. doi:10.1016/j.febslet.2011.02.005.

Wenzel RP. 1995. Nosocomial candidemia: risk factors and attributable mortality. Clin Infect Dis. 20(6):1531–1534. doi:10.1093/clinids/20.6.1531.

Wey SB, Mori M, Pfaller MA, Woolson RF, Wenzel RP. 1988. Hospital-acquired candidemia. The attributable mortality and excess length of stay. Arch Intern Med. 148(12):2642–2645. doi:10.1001/archinte.1988.00380120094019.

Wickham H., 2017 tidyverse: Easily Install and Load the "Tidyverse." R Package Version 1.2.1 https://CRAN.R-project.org/package=tidyverse.

Wu W, Lockhart SR, Pujol C, Srikantha T, Soll DR. 2007. Heterozygosity of genes on the sex chromosome regulates *Candida albicans* virulence. Mol Microbiol. 64(6):1587–1604. doi:10.1111/j.1365-2958.2007.05759.x.

Xie J, Tao L, Nobile CJ, Tong Y, Guan G, Sun Y, Cao C, Hernday AD, Johnson AD, Zhang L, *et al.* 2013. White–opaque switching in natural MTLa/α isolates of *Candida albicans*: evolutionary implications for roles in host adaptation, pathogenesis, and sex. PLoS Biol. 11(3):e1001525. doi:10.1371/journal.pbio.1001525.

Zeidler U, Lettner T, Lassnig C, Müller M, Lajko R, Hintner H, Breitenbach M, Bito A. 2009. *UME6* Is a crucial downstream target of other transcriptional regulators of true hyphal development in *Candida albicans*. FEMS Yeast Res. 9(1):126–142. doi:10.1111/j.1567-1364.2008.00459.x.

Ziv N, Brenes LR, Johnson A. 2022. Multiple molecular events underlie stochastic switching between 2 heritable cell states in fungi. PLoS Biol. 20(5):e3001657. doi:10.1371/journal.pbio.3001657.

Znaidi S, Nesseir A, Chauvel M, Rossignol T, d'Enfert C. 2013. A comprehensive functional portrait of two heat shock factor-type transcriptional regulators involved in *Candida albicans* morphogenesis and virulence. PLoS Pathog. 9(8):e1003519. doi:10.1371/journal.ppat.1003519.

Zordan RE, Galgoczy DJ, Johnson AD. 2006. Epigenetic properties of white–opaque switching in *Candida albicans* are based on a self-sustaining transcriptional feedback loop. Proc Natl Acad Sci USA. 103(34):12807–12812. doi:10.1073/pnas.0605138103.

Zordan R, Miller M, Galgoczy D, Tuch B, Johnson A. 2007. Interlocking transcriptional feedback loops control white–opaque switching in *Candida albicans*. PLoS Biol. 5(10):e256. doi:10.1371/journal.pbio.0050256.

Editor: L. Cowen